

Assessment of an energy-based surface tension model for simulation of two-phase flows using second-order phase field methods

Shahab Mirjalili^{a,*}, Makrand A. Khanwale^a, Ali Mani^a

^aCenter for Turbulence Research, Stanford University, Stanford, CA 94305, USA

Abstract

Second-order phase field models have emerged as an attractive option for capturing the advection of interfaces in two-phase flows. Prior to these, the state of the art models based on the Cahn-Hilliard equation, which is a fourth order equation, allowed for derivation of surface tension models through thermodynamic arguments. In contrast, the second-order phase field models do not follow a known energy law, and deriving a surface tension term for these models using thermodynamic arguments is not straight-forward. In this work, we justify that the energy-based surface tension model from the Cahn-Hilliard context can be adopted for second-order phase field models as well, and assess its performance. We test the surface tension model on three different second-order phase field equations; the conservative diffuse interface model of Chiu and Lin [1], and two models based on the modified Allen-Cahn equation introduced by Sun and Beckermann [2]. Using canonical tests, we illustrate the lower magnitude of spurious currents, better accuracy, and superior convergence properties of the energy-based surface tension model compared to the continuum surface force (CSF) model, which is a popular choice that is used in conjunction with second order phase field methods. Importantly, in terms of computational expense and parallel efficiency, the energy-based model incurs no penalty compared to the CSF model.

Keywords: two-phase flow, phase field, surface tension, diffuse interface, continuous surface force, Allen-Cahn

1. Introduction

In recent years, there has been considerable interest in second-order phase field equations that are suitable for modeling two-phase flows [2, 1, 3, 4]. Unlike models based on the Cahn-Hilliard equation [5, 6], these equations are not derived from an underlying thermodynamic basis, and as a result, it is difficult to derive energy-based surface tension terms for these models. Based on the second law of thermodynamics, the Korteweg stress tensor has been used successfully to model surface tension effects in the context of Cahn-Hilliard models [6, 7]. In this work, starting from the Korteweg stress tensor, we derive an energy-based surface tension force model for second order phase field equations. Using canonical test problems on three different phase field equations, we show that the proposed model has better properties than the continuum surface model (CSF), which is the highly explored alternative [8, 1, 9]. Specifically, the proposed model (1) is accurate and generates low spurious currents, (2) requires lower regularity compared to the direct implementation of Korteweg stress tensor, (3) does not require computation of curvature, (4) is amenable

*Corresponding author

Email addresses: ssmirjal@stanford.edu (Shahab Mirjalili), khanwale@stanford.edu (Makrand A. Khanwale), alimani@stanford.edu (Ali Mani)

to wide range of spatio-temporal discretization schemes.

2. Model derivation

To derive the energy-based surface tension model, let us consider a general phase field equation for incompressible flows in the form given by,

$$\frac{\partial \phi}{\partial t} + \frac{\partial}{\partial x_j} (u_j \phi) = g(\phi, \mathbf{x}). \quad (1)$$

The role of $g(\phi, \mathbf{x})$ is to regularize the interface. Traditional phase field models derive this right hand side term such that it minimizes a free energy functional. Most commonly, the Ginzburg-Landau free energy is utilized, corresponding to the chemical potential μ [10, 6] given by,

$$\mu = \frac{\hat{\sigma}}{\epsilon} \psi' - \hat{\sigma} \epsilon \frac{\partial}{\partial x_j} \left(\frac{\partial \phi}{\partial x_j} \right) \quad \text{where, } \psi = \frac{1}{2} [\phi(1 - \phi)]^2 \quad \text{and } \psi' = \phi(1 - \phi)(1 - 2\phi). \quad (2)$$

ϵ is the interfacial thickness parameter, and ψ is the free energy for a phase field variable, $\phi \in [0, 1]$. Additionally, $\hat{\sigma}$ is a constant related to surface energy, given by $\hat{\sigma} = 6\sigma^1$, where σ is the surface tension coefficient. In the special case of Allen-Cahn model we would have $g(\phi, \mathbf{x}) = -\mu$. Note that the Allen-Cahn equation admits an energy dissipation law similar to the Cahn-Hilliard equation. However, the lack of mass conservation, in addition to the curvature-driven flow it generates, render it unsuitable for simulation of two-phase flows, motivating the introduction of the alternative second-order phase field models we consider herein [2, 1, 9].

Historically, models based on the Cahn-Hilliard equation, where $g(\phi, \mathbf{x}) = \nabla^2 \mu$, have been used for simulation of two-phase flows. In this context, one can derive a surface tension model through the second law of thermodynamics. The surface tension force in this model is proportional to the divergence of the so called Korteweg stress tensor, $\frac{\partial}{\partial x_j} \left(\frac{\partial \phi}{\partial x_i} \frac{\partial \phi}{\partial x_j} \right)$, which prescribes an energy dissipation law [11, 6, 12, 7]. However, the more recently introduced second-order phase field equations for simulating interfacial flows do not admit an energy dissipation law as they are not gradient flows to any known energy functional. As such, these equations have typically been coupled to the momentum transport equation via the CSF model, $F_i = \sigma \kappa \frac{\partial \phi}{\partial x_i}$, where κ is the curvature [1, 9], defined as

$$\kappa = -\frac{\partial}{\partial x_j} \left(\frac{\frac{\partial \phi}{\partial x_j}}{\left(\frac{\partial \phi}{\partial x_k} \frac{\partial \phi}{\partial x_k} \right)^{1/2}} \right). \quad (3)$$

In this work, we return to the Korteweg stress tensor to assess its suitability for second-order phase field equations. Due to better regularity, flexibility offered in numerical discretization, and well-balancedness of volumetric surface tension models compared to integral formulations [13], we utilize the equivalent [14] surface tension force model,

$$F_i = \mu \frac{\partial \phi}{\partial x_i}. \quad (4)$$

¹Note that for Cahn-Hilliard models, instead of the factor 6 we have the factor of $3/2\sqrt{2} \approx 1$. This difference is due to the difference of the equilibrium profile of ϕ in the Cahn-Hilliard based models given by $\tanh\left(\frac{s}{\sqrt{2}\epsilon}\right)$ and $\phi \in [-1, 1]$, in contrast to $1/2 + \tanh(s/2\epsilon)$ and $\phi \in [0, 1]$ for phase field models considered here (s is the signed distance from the interface).

While this surface tension force model has been used and derived in the literature for Cahn-Hilliard models [5, 14, 6, 7], for completeness of narrative, we reproduce its derivation here. Starting from the surface tension force based on the Korteweg stress tensor, and using product rule:

$$\begin{aligned}\hat{\sigma}\epsilon\frac{\partial}{\partial x_j}\left(\frac{\partial\phi}{\partial x_i}\frac{\partial\phi}{\partial x_j}\right) &= \hat{\sigma}\epsilon\frac{\partial\phi}{\partial x_i}\left(\frac{\partial}{\partial x_j}\left(\frac{\partial\phi}{\partial x_j}\right)\right) + \hat{\sigma}\epsilon\frac{\partial\phi}{\partial x_j}\left(\frac{\partial}{\partial x_j}\left(\frac{\partial\phi}{\partial x_i}\right)\right) \\ &= \hat{\sigma}\epsilon\frac{\partial\phi}{\partial x_i}\left(\frac{\partial}{\partial x_j}\left(\frac{\partial\phi}{\partial x_j}\right)\right) + \hat{\sigma}\epsilon\frac{1}{2}\frac{\partial}{\partial x_i}\left(\frac{\partial\phi}{\partial x_j}\frac{\partial\phi}{\partial x_j}\right).\end{aligned}\quad (5)$$

We manipulate this expression to write it in terms of the chemical potential:

$$\begin{aligned}\hat{\sigma}\epsilon\frac{\partial}{\partial x_j}\left(\frac{\partial\phi}{\partial x_i}\frac{\partial\phi}{\partial x_j}\right) &= \hat{\sigma}\epsilon\frac{\partial\phi}{\partial x_i}\left(\frac{\partial}{\partial x_j}\left(\frac{\partial\phi}{\partial x_j}\right)\right) + \hat{\sigma}\epsilon\frac{1}{2}\frac{\partial}{\partial x_i}\left(\frac{\partial\phi}{\partial x_j}\frac{\partial\phi}{\partial x_j}\right) + \hat{\sigma}\epsilon\frac{\psi'}{\epsilon^2}\frac{\partial\phi}{\partial x_i} - \hat{\sigma}\epsilon\frac{\psi'}{\epsilon^2}\frac{\partial\phi}{\partial x_i}, \\ &= \frac{\partial\phi}{\partial x_i}\left(\frac{\hat{\sigma}}{\epsilon}\epsilon^2\frac{\partial}{\partial x_j}\left(\frac{\partial\phi}{\partial x_j}\right) - \frac{\hat{\sigma}}{\epsilon}\psi'\right) + \hat{\sigma}\epsilon\frac{1}{2}\frac{\partial}{\partial x_i}\left(\frac{\partial\phi}{\partial x_j}\frac{\partial\phi}{\partial x_j}\right) + \hat{\sigma}\epsilon\frac{\psi'}{\epsilon^2}\frac{\partial\phi}{\partial x_i}.\end{aligned}\quad (6)$$

The expression in the parenthesis in the first term can be replaced using the definition of μ eq. (2), which leads to:

$$\begin{aligned}\hat{\sigma}\epsilon\frac{\partial}{\partial x_j}\left(\frac{\partial\phi}{\partial x_i}\frac{\partial\phi}{\partial x_j}\right) &= -\mu\frac{\partial\phi}{\partial x_i} + \hat{\sigma}\epsilon\frac{1}{2}\frac{\partial}{\partial x_i}\left(\frac{\partial\phi}{\partial x_j}\frac{\partial\phi}{\partial x_j}\right) + \hat{\sigma}\epsilon\frac{\psi'}{\epsilon^2}\frac{\partial\phi}{\partial x_i}, \\ &= -\mu\frac{\partial\phi}{\partial x_i} + \frac{\partial}{\partial x_i}\left(\hat{\sigma}\epsilon\frac{1}{2}\frac{\partial\phi}{\partial x_j}\frac{\partial\phi}{\partial x_j} + \hat{\sigma}\frac{\psi}{\epsilon}\right).\end{aligned}\quad (7)$$

Recognize that the last term in eq. (7) can be absorbed in a redefined pressure. Therefore, the first term in eq. (7) can be used as a surface tension force in the momentum equations. Note that the sign of the surface tension force in eq. (7) is opposite of that of the Korteweg stress tensor. Additionally, the sign of $\mu\frac{\partial\phi}{\partial x_i}$ would be positive on the right hand side of the momentum equation.

2.1. Considered second-order phase field models

To ensure the generality of our conclusions, we examine the performance of the above energy-based surface tension force on three different second-order phase field equations. We consider (1) the conservative diffuse interface model, denoted by CDI [1, 3], (2) the modified Allen-Cahn model of Sun and Beckermann [2], denoted by SB, and (3) an implicit-capable second-order diffuse interface model we denote by ISODI. These equations are defined in Table 2.1.

Name	$g(\phi)$	Description
CDI	$\gamma \frac{\partial}{\partial x_j} \left[\epsilon \frac{\partial \phi}{\partial x_j} - \phi(1-\phi) \frac{\frac{\partial \phi}{\partial x_j}}{\left(\frac{\partial \phi}{\partial x_k} \frac{\partial \phi}{\partial x_k}\right)^{1/2}} \right]$	<i>Conservative Diffuse Interface (CDI) model [1, 3]</i>
Sun and Beckermann [2]	$\gamma \left[\epsilon \frac{\partial^2 \phi}{\partial x_j^2} - \frac{\phi(1-\phi)(1-2\phi)}{\epsilon} - \epsilon \left(\frac{\partial \phi}{\partial x_k} \frac{\partial \phi}{\partial x_k} \right)^{1/2} \frac{\partial}{\partial x_j} \left(\frac{\frac{\partial \phi}{\partial x_j}}{\left(\frac{\partial \phi}{\partial x_k} \frac{\partial \phi}{\partial x_k}\right)^{1/2}} \right) \right]$	Curvature subtracted Allen-Cahn based model proposed in Sun and Beckermann [2]
ISODI	$\gamma \left[\epsilon \frac{\partial^2 \phi}{\partial x_j^2} - \frac{\phi(1-\phi)(1-2\phi)}{\epsilon} - \phi(1-\phi) \frac{\partial}{\partial x_j} \left(\frac{\frac{\partial \phi}{\partial x_j}}{\left(\frac{\partial \phi}{\partial x_k} \frac{\partial \phi}{\partial x_k}\right)^{1/2}} \right) \right]$	<i>Implicit capable Second Order Diffuse Interface (ISODI) is a modification of model in Sun and Beckermann [2] for full time-implicit schemes</i>

Note that the ISODI model is derived by modifying the third term in the model by Sun and Beckermann [2] using the equilibrium relation $(\partial \phi / \partial x_k \partial \phi / \partial x_k)^{1/2} = \phi(1-\phi) / \epsilon$. This allows for an easier setup of Newton iteration for fully-implicit schemes.

2.2. Equivalence with a modified continuum surface force model

Before implementing the model proposed in (4), we present further analysis of its right hand side to generate some insight regarding its connection and contrast compared to CSF. For second-order phase field equations considered in this work, at equilibrium, the energy-based surface tension model (eq. (4)) is analytically equivalent to a modified CSF model given by $F_i = \hat{\sigma} \kappa \phi(1-\phi) \frac{\partial \phi}{\partial x_i}$. To prove this, note that at equilibrium, all three models in section 2.1 yield a hyperbolic tangent profile in the direction normal to the interface, whereby

$$\left(\frac{\partial \phi}{\partial x_k} \frac{\partial \phi}{\partial x_k} \right)^{1/2} = \frac{\phi(1-\phi)}{\epsilon} \quad (8)$$

Also, note that, at equilibrium ($g(\phi) = 0$), for the three models presented in section 2.1, using eq. (8), we have the following equation²,

$$\epsilon \frac{\partial^2 \phi}{\partial x_j^2} - \frac{\phi(1-\phi)(1-2\phi)}{\epsilon} = -\kappa \phi(1-\phi). \quad (9)$$

Now multiplying by $\hat{\sigma}$ and using the definition of μ (eq. (2)),

$$-\mu = \hat{\sigma} \epsilon \frac{\partial^2 \phi}{\partial x_j^2} - \hat{\sigma} \frac{\phi(1-\phi)(1-2\phi)}{\epsilon} = -\hat{\sigma} \kappa \phi(1-\phi). \quad (10)$$

Now using eq. (9) and multiplying by $-\frac{\partial \phi}{\partial x_i}$ we get,

$$\mu \frac{\partial \phi}{\partial x_i} = \hat{\sigma} \kappa \phi(1-\phi) \frac{\partial \phi}{\partial x_i} = \hat{\sigma} \kappa \epsilon \left(\frac{\partial \phi}{\partial x_k} \frac{\partial \phi}{\partial x_k} \right)^{1/2} \frac{\partial \phi}{\partial x_i}. \quad (11)$$

²For CDI, here we expand the $g(\phi)$ to get $\epsilon \frac{\partial^2 \phi}{\partial x_j^2} - \left(\frac{\partial \phi}{\partial x_k} \frac{\partial \phi}{\partial x_k} \right)^{1/2} \frac{(1-2\phi)}{\epsilon} + \phi(1-\phi) \kappa$

It is important to note that in the right hand side of eq. (11), the factor of $\phi(1 - \phi) = \epsilon \left(\frac{\partial \phi}{\partial x_k} \frac{\partial \phi}{\partial x_k} \right)^{1/2}$ modifies the popular CSF model ($\hat{\sigma} \kappa \partial \phi / \partial x_i$) with a regularization kernel which is localized near the interface. The numerical results below confirm that this localization improves the accuracy of the surface tension model compared to the original CSF model.

3. Results and discussion

In this section, using canonical tests, we numerically test the proposed surface tension model by comparing its performance against the CSF model. We use second-order finite differences on a staggered Cartesian grid in space and RK4 time-integration, as described in Mirjalili and Mani [9].

3.1. Spurious currents

We consider a standard 2D benchmark for testing spurious currents generated by two-phase flow solvers [15, 16, 17]. In a 1×1 domain with free-slip boundary conditions, at $t = 0$, a circular drop with diameter $D = 0.4$ is placed in the center of the domain with $\vec{u} = 0$ everywhere. The density and viscosity of the two phases are equal, $\rho_1 = \rho_2 = 300$ and $\mu_1 = \mu_2 = 0.1$, the surface tension coefficient is $\sigma = 0.1$, and the dimensionless parameter characterizing this problem is the Laplace number, $La = \sigma \rho D / \mu^2 = 12000$. Any sustained flow in the numerical solution is due to errors in computing the surface tension force. We examine $Ca_\infty = (\|\vec{u}\|_\infty \sigma) / \mu$ at non dimensional time $t^* = \sigma t / (\mu D) = 250$, which is a large enough time for the surface tension and viscous forces to have balanced each other and for spurious currents to be fully developed [17, 18].

Panel (a) of fig. 1 shows the convergence of Ca_∞ as we increase the number of mesh points ($N \times N$) for a fixed interfacial thickness, $\epsilon = 1/32$. By successively refining the mesh, this analysis illustrates the property of the models in the continuous limit, thereby teasing out the PDE errors. It is clear that for all three chosen phase field equations, the proposed energy-based model (denoted with EB) outperforms CSF due to a better convergence order (second order versus first order of CSF).

Panel (b) of fig. 1 shows the convergence of Ca_∞ as we approach the sharp-interface limit. An important property of a physical model is to converge to true sharp interface physics as $\epsilon \rightarrow 0$. As we reduce ϵ , we refine the mesh via $\Delta x = 32^{1/2} \epsilon^{3/2}$ [5, 18]. In practice, to allow an integer number of mesh points, we successively refine the mesh by a factor of two while computing ϵ proportional to $\Delta x^{2/3}$. We observe that for all three phase field equations, the proposed model converges faster (second order) to the sharp interface limit compared to the CSF model (first order). A faster convergence to the sharp interface limit has practical benefit in terms of computational resource requirements, as it allows for choice of larger ϵ values which usually requires coarser spatio-temporal resolutions.

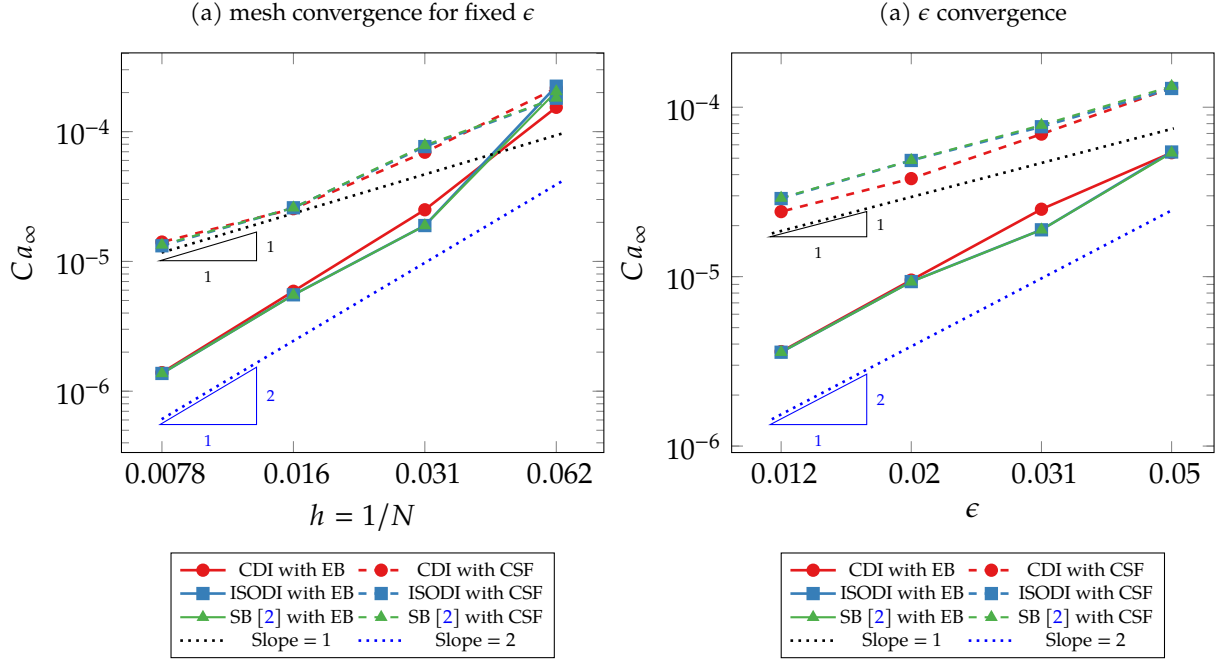


Figure 1: *Section 3.1 Spurious currents*: Comparison of convergence of spurious currents generated by the the proposed energy-based surface tension model (denoted by EB in the legend) and CSF model. Panel (a) shows mesh convergence of Ca_∞ for a fixed ϵ ; Panel (b) shows convergence of Ca_∞ as ϵ approaches the sharp interface limit. Solid lines are used to denote results for the proposed energy-based surface tension and dashed lines are used to denote results for CSF model.

3.2. Standing Wave

By examining surface oscillations of a standing wave, one can assess the accuracy of a two-phase flow solver in capturing interactions among inertial, capillary, and viscous forces [19, 17, 18]. We compare the accuracy of the proposed surface tension model against the CSF model in capturing the amplitude of a 2D standing wave as a function of time. In a $2\pi \times 2\pi$ domain with periodic boundary conditions in the x direction and free-slip on the top and bottom walls, at $t = 0$, a small-amplitude wave is placed between two immiscible phases. The initial wave height is $h_{\text{wave}}(x, t = 0) = y - y_0 + A_0 \cos(x - \Delta x/2)$, where $y_0 = \pi$ and $A_0 = 2\pi/100$. The surface tension is $\sigma = 2$, density of the two phases is $\rho_1 = \rho_2 = 1$, kinematic viscosity of both phases is $\nu_1 = \nu_2 = 0.064720863$, and the time step is $\Delta t = 0.003$. We measure the amplitude of the standing wave at $x = \Delta x/2$ as a function of time.

Panels (a), (b), and (c) of fig. 2 depict the normalized surface wave amplitude (A/λ) as a function of time for simulations performed using CDI, ISODI, and SB phase field methods respectively. For panels (a), (b), and (c) of fig. 2 we fix the value of $\epsilon = 1/32$ and vary the mesh resolution. We compare the performance of the proposed surface tension model against CSF, and the exact solution (see Prosperetti [20]) for each resolution. Notice that for all three models (panels (a), (b), and (c)), the proposed surface tension model (solid lines and denoted by EB) outperforms CSF (dashed lines and denoted by CSF) when compared against the exact solution (except for the lowest resolution simulations with 16×16 mesh points). Additionally, it is important to note that as we refine the mesh, both CSF and the proposed surface tension model converge to a solution, which implies a minimization of the spatial discretization error. Therefore, for the highest resolution we are predominantly observing a PDE error caused by the choice of a finite ϵ . If we then inspect the converged solutions (purple solid line for proposed surface tension model and purple dashed line for CSF model), it is clear that the PDE-level error committed using the energy-based surface ten-

sion model is much smaller than that of the CSF model for all three phase field methods (panels (a), (b), and (c)). Therefore, we can infer from results of panels (a), (b), and (c) that the proposed surface tension model has a smaller PDE error compared to CSF for a fixed ϵ .

Panel (d) of fig. 2 illustrates the convergence of the l^2 error computed between the surface wave amplitude and the theoretical solution [20] as we approach the sharp interface limit (i.e. $\epsilon \rightarrow 0$). While reducing ϵ , we refine the mesh via $\Delta x = 32^{1/2}\epsilon^{3/2}$. For all three phase field equations, we observe that the energy-based surface tension force model (symbols with solid lines) is more accurate than CSF (symbols with dashed lines) while maintaining its convergence order of one.

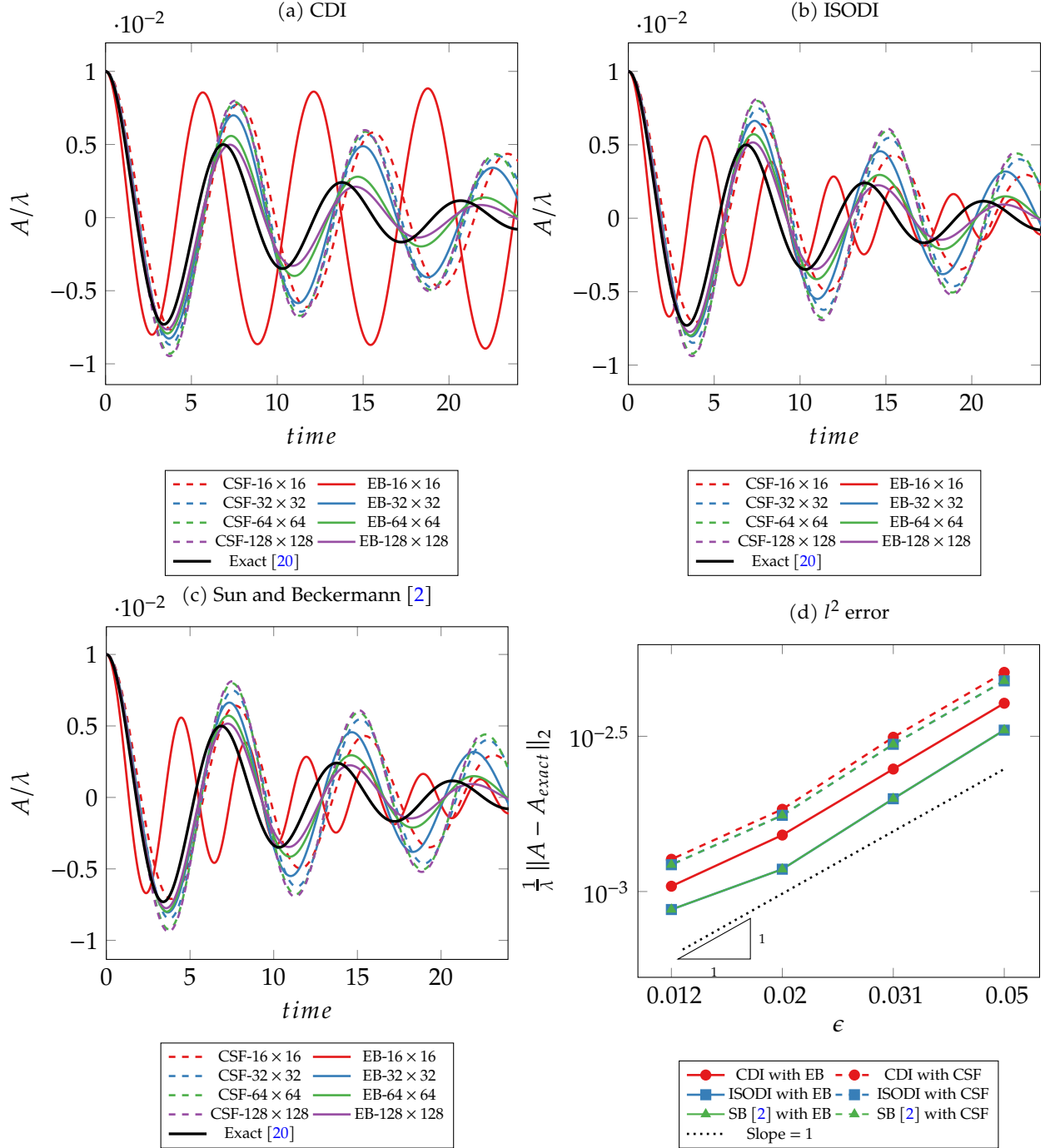


Figure 2: *Section 3.2 Standing Wave*: Comparison of accuracy of capturing surface oscillations of a standing wave with the proposed energy-based surface tension model (denoted by EB in the legend) and the CSF model. Panel (a) shows comparison of the surface oscillations between the proposed surface tension model (EB), CSF, and the theoretical solution [20] for CDI phase field model (see 2.1 for details) with varying mesh resolution for a fixed ϵ ; Panel (b) shows same analysis as in panel (a) but with the ISODI phase field model (see 2.1 for details); Panel (c) shows same analysis as in panel (a) but with the model from Sun and Beckermann [2] (see 2.1 for details); Panel (d) shows convergence of l^2 error between the surface oscillation and theoretical solution [20] with respect to the interface thickness ϵ for the proposed surface tension model (EB) and CSF for all three phase field models analysed in panels (a), (b), and (c). In all four panels solid lines are used to denote results for the proposed surface tension (EB) and dashed lines are used to denote results for the CSF model.

4. Summary and perspective

In this work, we provided theoretical justification for the use of eq. (4) as an energy-based surface tension force model in conjunction with second-order phase field models. Through extensive testing on two canonical problems, we revealed the relative accuracy of the proposed surface tension model compared to CSF. These two cases allowed us to assess the accuracy of the model to capture static equilibrium solutions and dynamic interactions involving the interplay of surface tension forces with inertial and viscous forces. We observed from fig. 1 that the proposed model leads to a faster rate of decay for spurious currents (second order) with respect to mesh resolution and interfacial thickness ϵ (the sharp interface limit) as compared to the CSF (first order). This is analogous to observations from the Cahn-Hilliard model [5] and is intuitively expected since the equilibrium solution of the second-order phase field models is also a hyperbolic tangent. Additionally, from fig. 2 we observed that the proposed surface tension model is more accurate compared to the CSF model in dynamically active scenarios involving exchanges between various modes of energy. This improved performance can be interpreted via the equivalence of the proposed surface tension model with a localized CSF model (eq. (11)), discussed in section 2.2. Both of these properties are highly sought after for accurate two-phase flow simulations. While our tests were two dimensional, our findings can be readily generalized to three-dimensional settings. With this short note, we propose the model presented in eq. (4) as an alternative to the CSF model for surface tension forces in two-phase flow simulations that utilize second-order phase field equations.

5. Acknowledgements

We acknowledge financial support from the Office of Naval Research (Grant N00014-15-1-2523) and Palo Alto Research Center (Grant 249996). The computations in this note were performed on the Yellowstone cluster at the Stanford HPC Center, supported through awards from Intel, National Science Foundation, DOD HPCMP, and Office of Naval Research.

References

- [1] P.-H. Chiu, Y.-T. Lin, A conservative phase field method for solving incompressible two-phase flows, *Journal of Computational Physics* 230 (2011) 185–204.
- [2] Y. Sun, C. Beckermann, Sharp interface tracking using the phase-field equation, *Journal of Computational Physics* 220 (2007) 626–653.
- [3] S. Mirjalili, C. B. Ivey, A. Mani, A conservative diffuse interface method for two-phase flows with provable boundedness properties, *Journal of Computational Physics* 401 (2020) 109006.
- [4] Z. Huang, G. Lin, A. M. Ardekani, Consistent and conservative scheme for incompressible two-phase flows using the conservative allen-cahn model, *Journal of Computational Physics* 420 (2020) 109718.
- [5] D. Jacqmin, Calculation of two-phase navier-stokes flows using phase-field modeling, *Journal of Computational Physics* 155 (1999) 96–127.
- [6] H. Abels, H. Garcke, G. Grün, Thermodynamically consistent, frame indifferent diffuse interface models for incompressible two-phase flows with different densities, *Mathematical Models and Methods in Applied Sciences* 22 (2012) 1150013.

- [7] M. A. Khanwale, A. D. Lofquist, H. Sundar, J. A. Rossmannith, B. Ganapathysubramanian, Simulating two-phase flows with thermodynamically consistent energy stable cahn-hilliard navier-stokes equations on parallel adaptive octree based meshes, *Journal of Computational Physics* 419 (2020) 109674.
- [8] J. U. Brackbill, D. B. Kothe, C. Zemach, A continuum method for modeling surface tension, *Journal of Computational Physics* 100 (1992) 335–354.
- [9] S. Mirjalili, A. Mani, Consistent, energy-conserving momentum transport for simulations of two-phase flows using the phase field equations, *Journal of Computational Physics* 426 (2021) 109918.
- [10] M. E. Gurtin, Generalized ginzburg-landau and cahn-hilliard equations based on a microforce balance, *Physica D: Nonlinear Phenomena* 92 (1996) 178–192.
- [11] J. Shen, X. Yang, A phase-field model and its numerical approximation for two-phase incompressible flows with different densities and viscosities, *SIAM Journal on Scientific Computing* 32 (2010) 1159.
- [12] Z. Guo, P. Lin, J. Lowengrub, S. M. Wise, Mass conservative and energy stable finite difference methods for the quasi-incompressible navier–stokes–cahn–hilliard system: Primitive variable and projection-type schemes, *Computer Methods in Applied Mechanics and Engineering* 326 (2017) 144–174.
- [13] S. Popinet, Numerical models of surface tension, *Annual Review of Fluid Mechanics* 50 (2018) 49–75.
- [14] J. Kim, A continuous surface tension force formulation for diffuse-interface models, *Journal of Computational Physics* 204 (2005) 784–804.
- [15] M. Williams, D. Kothe, E. Puckett, Accuracy and convergence of continuum surface tension models, *Fluid Dynamics at Interfaces*, Cambridge University Press, Cambridge (1998) 294–305.
- [16] M. M. François, S. J. Cummins, E. D. Dendy, D. B. Kothe, J. M. Sicilian, M. W. Williams, A balanced-force algorithm for continuous and sharp interfacial surface tension models within a volume tracking framework, *Journal of Computational Physics* 213 (2006) 141–173.
- [17] M. Herrmann, A balanced force refined level set grid method for two-phase flows on unstructured flow solver grids, *Journal of Computational Physics* 227 (2008) 2674–2706.
- [18] S. Mirjalili, C. B. Ivey, A. Mani, Comparison between the diffuse interface and volume of fluid methods for simulating two-phase flows, *International Journal of Multiphase Flow* 116 (2019) 221–238.
- [19] D. Gerlach, G. Tomar, G. Biswas, F. Durst, Comparison of volume-of-fluid methods for surface tension-dominant two-phase flows, *International Journal of Heat and Mass Transfer* 49 (2006) 740–754.
- [20] A. Prosperetti, Motion of two superposed viscous fluids, *Phys. Fluids* 24 (1981) 1217–1223.